Am J Transl Res 2021;13(11):12509-12522
www.ajtr.org /ISSN:1943-8141/AJTR0137667

Original Article

Intercellular transport of Tau protein and β-amyloid mediated by tunneling nanotubes

Kejia Zhang[1], Zehui Sun[1], Xinyu Chen[1], Yifan Zhang[1], Angyang Guo[3], Yan Zhang[1,2]

[1]*State Key Laboratory of Membrane Biology, College of Life Sciences, Peking University, Beijing 100871, China;* [2]*PKU-IDG/McGovern Institute for Brain Research, Beijing 100871, China;* [3]*Duke Kunshan University, Kunshan 215316, Jiangsu, China*

Received July 24, 2021; Accepted September 5, 2021; Epub November 15, 2021; Published November 30, 2021

Abstract: Tunneling nanotubes (TNTs) are thin channel-like structures connecting distant cells, providing a route for intercellular communication. In this study, we investigated the physical properties, including the cytoskeletal components, length and diameter, of the TNTs formed by HEK293T, U87 MG, and U251 cell lines. We found that organelles such as lysosomes, mitochondria, and Golgi bodies can be transported through TNTs, indicating that TNTs can mediate material transport. Moreover, we investigated the transport of the Tau protein and β-amyloid (Aβ), which are both closely related to Alzheimer's disease (AD) pathology, through TNTs. The results showed that TNTs formed by various neuronal cell lines can mediate the transport of different forms of the Tau protein and fluorescently labeled Aβ and that this transport is bidirectional, with different velocities in various cell lines. Our results confirmed the transport of the Tau protein and Aβ between cells and provided a possible explanation for the cascade of cell death in specific brain regions during the progression of AD. Our findings suggest new possibilities for the treatment of AD.

Keywords: Alzheimer's disease, tunneling nanotubes, Tau protein, β-amyloid

Introduction

Communication between cells is essential for single-cell and multicellular organisms because it enables the regulation of complex physiologic processes such as homeostasis and development. Cell-to-cell communication is achieved through soluble factors involved in endocrine and paracrine signaling and through cell-to-cell contact and is mediated by gap junctions, synapses (neural and immune), and plasmodesmata [1]. In addition to the above-mentioned cell-to-cell communication, long-distance cell-to-cell communication composed of different types of membrane extensions (called tunneling nanotubes) *in vitro* has been extensively described [2].

TNTs are considered novel modalities of communication between cells [3]. In contrast to other forms of cell-to-cell communication, TNTs are membrane channel structures that directly connect the cytoplasm of two cells not in direct contact with each other and that can mediate cell-to-cell communication. TNT-like structures have been observed in different types of cells [4]. A growing number of studies have shown that TNTs play a powerful role in intercellular communication. It has been reported that a variety of cellular molecules and organelles, such as proteins, vesicles, mitochondria, Golgi bodies, and lysosomes, can be transported through TNTs [5, 6]. In addition, pathogens can be transported from infected cells to healthy cells through TNTs, including prions, HIV, and influenza viruses [7-9]. Studies have also shown that TNTs are associated with gap junctions, which allow electrical coupling between remotely positioned cells [10]. TNT-mediated signal transduction and organelle transport play important roles in both physiologic and pathologic states [11]. Under physiologic conditions, TNTs are involved in cell reprogramming, cell differentiation, and attenuation of mitochondrial dysfunction, senescence and angiogenesis [12-16]. Under pathologic conditions, TNTs promote the progression of diseases such as neurodegenerative diseases, acquired immune deficiency syndrome (AIDS), and cancer [7, 17-19].

One of the most common functions of TNTs in diseases is the mediation of transport of pathogens, including prions, bacteria, and viruses [4]. Protein aggregates are pathological markers of many neurodegenerative diseases, such as Alzheimer's disease (AD), Huntington's disease (HD), Parkinson's disease (PD), and amyotrophic lateral sclerosis (ALS) [20, 21]. The spread of protein aggregates in the brain is believed to be associated with the development of neurodegenerative diseases, and protein aggregation is associated with neuronal dysfunction [22]. However, the exact mechanism underlying the spread of pathogenic protein aggregates is not fully understood. In an example of protein aggregate spreading, α-synuclein is transported from one cell to another through TNTs. It has been reported that α-synuclein in lysosomes is effectively transported between nerve cells through TNTs, with soluble α-synuclein transported into recipient cells forming aggregates that serve as seed proteins that are subsequently redistributed [23]. More importantly, different disease-associated proteins have been found to support TNT-mediated transport of pathogenic protein aggregates [18, 24-26]. Taken together, these results suggest that TNT may be a common mechanism by which neurodegenerative diseases develop, providing a target for the treatment of these diseases.

Regarding AD pathogenesis, aggregates of the β-amyloid (Aβ) and Tau proteins are the two most common causes of AD [27]. In the Aβ hypothesis, Aβ dimers, oligomers, and plaques are the pathogenic sources of AD. The Tau protein hypothesis suggests that highly phosphorylated Tau protein causes the death of nerve cells, leading to the development of neurodegenerative diseases.

In this study, we investigated the function of TNTs in the central nervous system. Using time-lapse imaging technology, we demonstrated that Tau protein and Aβ can be transported at different velocities in various cell lines through TNTs. The results provide a possible explanation for the cascade of nerve cell death in the brain during AD development. Furthermore, we found that lysosomes, mitochondria, and Golgi bodies can be transported by TNTs, suggesting that TNTs can mediate material transport between cells.

Materials and methods

Cell culture and transfection

HEK293T, U87 MG, and U251 cells were dissociated in 0.05% trypsin (Invitrogen) for 2 minutes. After trypsinization, the same volume of Dulbecco's modified Eagle's medium (DMEM, Gibco) containing 10% fetal bovine serum (FBS, Gibco) was added to HEK293T cells, which were then centrifuged at 500×g for 2 minutes. The cells were resuspended in DMEM containing 10% FBS and plated on a coverslip coated with poly-D-lysine (Sigma). The cells were cultured in an incubator at 37°C with 5% CO_2.

To transfect the cells, 150 μL Opti-MEM, 20 μg of a plasmid solution, and 60 μL of Lipofectamine™ 2000 transfection reagent (Thermo Fisher Scientific) were mixed and incubated at room temperature for 30 minutes. The transfection mixture was added to the cell culture medium in 10-cm cell dishes and incubated at 37°C. Six hours later, the medium was changed to DMEM with 10% FBS and incubated at 37°C.

Western blotting

Cells were collected by radioimmunoprecipitation assay (RIPA) lysis buffer (R&D), and proteins were obtained by centrifugation. Bovine serum albumin (BSA, Sigma) was prepared at six concentrations (10 mg/mL, 5 mg/mL, 2.5 mg/mL, 1.25 mg/mL, 0.625 mg/mL, and 0.3125 mg/mL). The working solution was prepared following the instructions of a bicinchoninic acid (BCA) assay kit (Invitrogen). For the BCA assay, 200 μL of the working solution and 5 μL of protein lysate or standard solution were added to each well, mixed thoroughly and incubated at 37°C for 30 minutes. For all the protein samples, the absorbance values were measured at 562 nm with an enzyme plate analyzer. The protein sample concentration was calculated by linear fitting of the standard curve according to the concentration of the standard protein solution and absorbance. The proteins were denatured at 100°C for 5 minutes and separated by 10% sodium dodecyl sulfate-polyacrylamide gel electrophoresis (SDS-PAGE) at 80 mA for 2 hours. The proteins were transferred to a polyvinylidene fluoride (PVDF) membrane (Millipore) at 100 mA for 2 hours. The membrane was blocked with Tris-buffered saline (TBS, Sigma) containing 5% BSA and 0.1% Tween 20 (TBST) at room tem-

Table 1. Chemicals and antibodies

Chemicals and antibodies	Source	Dilution
CellTracker™ fluorescent probes	Invitrogen	1:1000
MitoTracker Mitochondrion probes	Invitrogen	1:2000
LysoTracker probes	Invitrogen	1:1000
CellLight Golgi-GFP	Invitrogen	1:100
Anti-F-actin antibody	Abcam	1:500
Anti-alpha tubulin antibody	Abcam	1:200
Anti-beta tubulin antibody	Abcam	1:200
Donkey anti-rabbit 488	Invitrogen	1:500
Donkey anti-mouse 488	Invitrogen	1:500
Donkey anti-chicken 488	Invitrogen	1:500
Donkey anti-rabbit 568	Invitrogen	1:500
Donkey anti-mouse 568	Invitrogen	1:500
Donkey anti-chicken 568	Invitrogen	1:500
Donkey anti-rabbit 647	Invitrogen	1:500
Donkey anti-mouse 647	Invitrogen	1:500
Donkey anti-chicken 647	Invitrogen	1:500
Anti-Flag	Sigma	1:500
Anti-β actin-HRP	EASY BIO	1:500
Anti-GAPDH-HRP	EASY BIO	1:500

perature for 1 hour. Antibody was diluted to an appropriate concentration and added to a 5% BSA solution prepared with TBST and incubated with the membrane overnight at 4°C. On the next day, the membrane was washed 3 times with TBST for 10 minutes each time, and a secondary antibody labeled with horseradish peroxidase (HRP) was added to the membrane, which was washed 3 times for 10 minutes each time, and the optical density of the HRP was detected by enhanced chemiluminescence. The optical density of the HRP was analyzed with a Bio-Rad ChemiDox imaging system (Bio-Rad).

Immunostaining and imaging

The cells were washed in phosphate-buffered saline (PBS, HyClone) and fixed in 4% paraformaldehyde (PFA, Sigma) for 20 minutes at room temperature. Then, the cells were infiltrated with 0.1% Triton at 4°C, blocked with 5% donkey serum at room temperature, and incubated with the primary antibody at 4°C for 24 hours. Twenty-four hours later, secondary antibody was added to the cells for 1 hour in the dark. The nuclei were stained with 4',6-diamino-2-phenylindole (DAPI, Sigma) for 15 minutes. Finally, the coverslip with the cells was placed on slides for imaging. All chemicals and antibodies were listed in **Table 1**.

Before the experiment, 2.0×10^4 cells were plated on a glass bottom dish (NEST) and incubated for 48 hours. Time-lapse imaging was performed with an inverted confocal microscope (Dragonfly, LeicaDMI8) and a MicroPoint laser workstation (Andor). Images were captured with a microscope (Dragonfly, LeicaDMI8) and analyzed with Imaris software.

Cloning and plasmids

$SpGFP_{1-10}$ and $spGFP_{11}$ plasmids were obtained from Dr. Yulong Li (Peking University), amplified by polymerase chain reaction (PCR), and cloned into pcDNA3.1. Tau-$spGFP_{1-10}$-pcDNA3.1 was constructed based on $spGFP_{1-10}$-pcDNA3.1. All constructs were verified by DNA sequencing. The plasmids were transfected into all cell lines using Lipofectamine™ 2000 transfection reagent (Thermo Fisher Scientific) according to the manufacturer's instructions.

Statistical evaluation

The dead cells shown in **Figure 1** are clearly distinguished by their notable morphologic characteristics, such as shrinkage and detachment from the substrate. GraphPad Prism 7.0 software was used for statistical analysis. Student's t test and two-way ANOVA were performed to assess the statistical significance between groups. A *P*-value less than 0.05 indicated statistical significance.

Results

Length, diameter, and cytoskeletal component of TNTs

In previous studies, TNT formation was shown to increase in cells under stress conditions such as oxidative stress, serum deprivation, pathogenic protein aggregation, and pathogen infection [28]. Therefore, in this study, we used H_2O_2 to induce the formation of TNTs by HEK-293T human embryonic kidney cells, U87 MG human astroblastoma cells, and U251 human glioma cells. The results showed that with increasing H_2O_2 concentration in HEK293T and U87 MG cells, TNT formation was gradually increased (**Figure 1A-D**). Compared with that of the control group, TNT formation was significantly increased in the cell groups treated with 100 μmol/L H_2O_2, and there was no significant change in the number of dead cells in the four

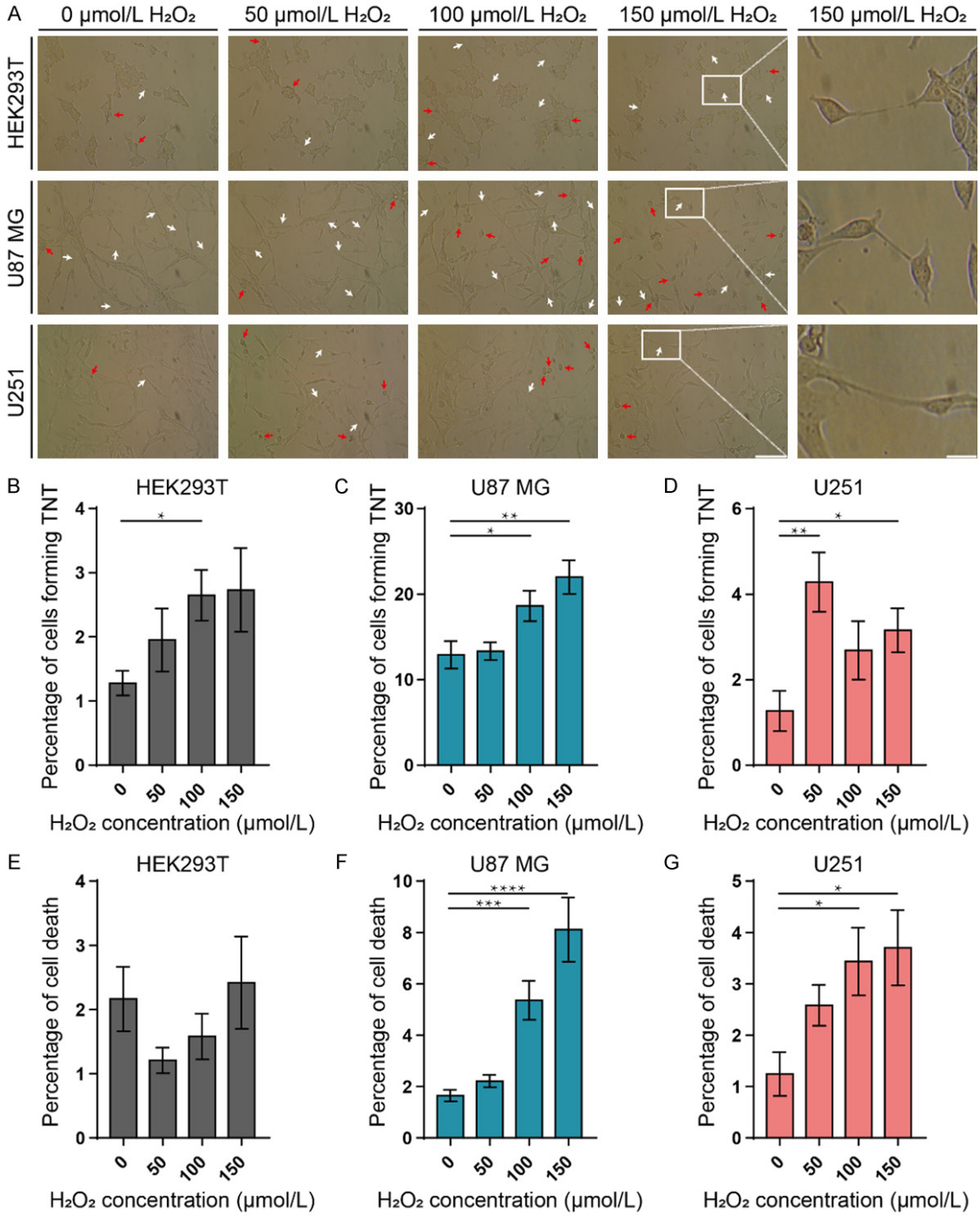

Figure 1. H_2O_2 induced TNT formation by HEK293T, U87 MG, and U251 cells. TNT formation was induced by different concentrations of H_2O_2 administered to HEK293T, U87 MG, and U251 cells. Based on a comprehensive analysis of the number of cells that formed TNTs and the number of dead cells in the treatment groups treated with different H_2O_2 concentrations, 100 μmol/L H_2O_2 was used to induce TNT formation by HEK293T and U87 MG cells, and 50 μmol/L H_2O_2 was used to induce TNT formation by U251 cells. A. Representative images of the TNTs produced by HEK293T, U87 MG, and U251 cells treated with 0, 50, 100, and 150 μmol/L H_2O_2. White arrowheads indicate TNTs between cells. Red arrowheads indicate dead cells. Objective: 10× and eyepiece: 10×. Scale bars: 30 μm (left) and 6 μm (right). B-D. The number of HEK293T, U87 MG, and U251 cells that formed TNTs after induction with gradient concentrations of H_2O_2, N=5 fields in each group. E-G. The number of dead HEK293T, U87 MG, and U251 cells after induction with gradient concentrations of H_2O_2, N=5 in each group. T test, $^{*}P<0.05$, $^{**}P<0.01$, $^{***}P<0.001$, $^{****}P<0.0001$.

groups of HEK293T cells (**Figure 1B**, **1E**). However, when U87 MG cells were treated with 100 and 150 μmol/L H_2O_2, the number of dead cells increased significantly (**Figure 1F**). In U251 cells, TNT formation induced by 50 μmol/L H_2O_2 was significantly increased (**Figure 1D**). With increasing H_2O_2 concentration, the number of dead cells increased gradually (**Figure 1G**). Considering this analysis of TNT formation and the number of dead cells at different concentrations of H_2O_2, we selected 100 μmol/L H_2O_2 to induce the formation of TNTs by HEK293T and U87 MG cells and 50 μmol/L H_2O_2 to induce TNT formation by U251 cells.

Previous studies reported that the cytoskeletal component of TNTs varies greatly in different cells, and whether TNTs contain microtubules remains a hotly debated issue [15, 29-32]. Therefore, we investigated the cytoskeletal components of TNTs in HEK293T, U87 MG, and U251 cells. Immunocytochemistry was performed in cells induced with the established working concentrations of H_2O_2 for 24 hours. The results showed that TNTs formed by the HEK293T, U87 MG, and U251 cells all contained cytoskeletal proteins, including F-actin, α-tubulin, and β-tubulin (**Figure 2A**).

In addition, we analyzed the length of the TNTs formed by the three cell lines. The results showed that the lengths of the TNTs formed by the HEK293T, U87 MG, and U251 cells were 35.44±1.856 μm, 43.15±1.875 μm, and 29.96±1.548 μm, respectively (**Figure 2B**). The diameter, measured from the middle of the TNTs in HEK293T cells (1.350±0.049 μm) was larger than that of the U87 MG cells (1.004±0.039 μm) and U251 cells (0.964±0.026 μm) (**Figure 2C**). The diameter at the terminus of a TNT in the U251 cells (1.683±0.049 μm) was smaller than that in the other two cell lines, and there was no significant difference in the terminal diameter between the HEK293T cells (2.187±0.082 μm) and U87 MG cells (2.067±0.067 μm) (**Figure 2D**).

TNTs play critical roles in intercellular communication. It has been recently discovered that various cytoplasmic components including mitochondria, vesicles, lysosomes, Golgi bodies, proteins, RNA particles, and even pathogens such as viruses and bacteria, can be transported between cells through TNTs [5-9]. Since TNT-mediated organelle transport is essential for cell survival, we next explored whether various organelles can be transported through TNTs formed by U87 MG and U251 cells. Lysosomes, mitochondria, and Golgi bodies were clearly observable in the TNTs of U87 MG and U251 cells (**Figure 2E**, **2F**). These results suggested that TNTs can mediate the intercellular transport of lysosomes, mitochondria, and Golgi bodies between U87 MG and between U251 cells, indicating that TNTs can mediate the intercellular transport of organelles between cells, especially under stress conditions.

The Tau-spGFP$_{1-10}$-pcDNA3.1 fusion protein can be transported between cells through TNTs

In 1907, Dr. Alois Alzheimer discovered the pathologic features of intracellular neurofibrillary tangles in dementia patients. In the 1980s, researchers found that formation of these tangles is mainly a result of the aggregation of hyperphosphorylated microtubule-associated Tau protein. However, at the time, the role of Tau protein in AD was not clear. We used spilt green fluorescent protein (spGFP) to verify the transport of Tau protein through TNTs. We first constructed Tau-spGFP$_{1-10}$-pcDNA3.1 (Tau-spGFP$_{1-10}$) and spGFP$_{11}$-pcDNA3.1 (spGFP$_{11}$) plasmids and verified their expression in HEK293T cells (Figure S1A). The results showed that the Tau-spGFP$_{1-10}$ and spGFP$_{11}$ plasmid genes were successfully expressed and that the encoded proteins possessed the structural characteristics of spGFP (Figure S1B). After confirming the expression of the Tau-spGFP$_{1-10}$ plasmid genes, donor cells were co-transfected with spGFP$_{1-10}$/Tau-spGFP$_{1-10}$ and mCherry and then cocultured for 48 hours with recipient cells labeled with CellTracker 647 and transfected with spGFP$_{11}$ (Figure S1C). Green fluorescence was observed in the recipient cells, and TNTs extended from both spGFP$_{1-10}$ and Tau-spGFP$_{1-10}$ donor cells, which suggested that Tau-spGFP$_{1-10}$ can be transported from cell to cell through TNTs and can react with spGFP$_{11}$ to produce green fluorescence (Figure S1D).

To further investigate the intercellular transport of the Tau-spGFP$_{1-10}$ protein through TNTs, we performed time-lapse imaging of living cells. HEK293T cells co-transfected with spGFP$_{1-10}$/Tau-spGFP$_{1-10}$ and mCherry were used as donor cells, and those co-transfected with spGFP$_{11}$ and blue fluorescent protein (BFP) were used as recipient cells. After 24 hours of transfec-

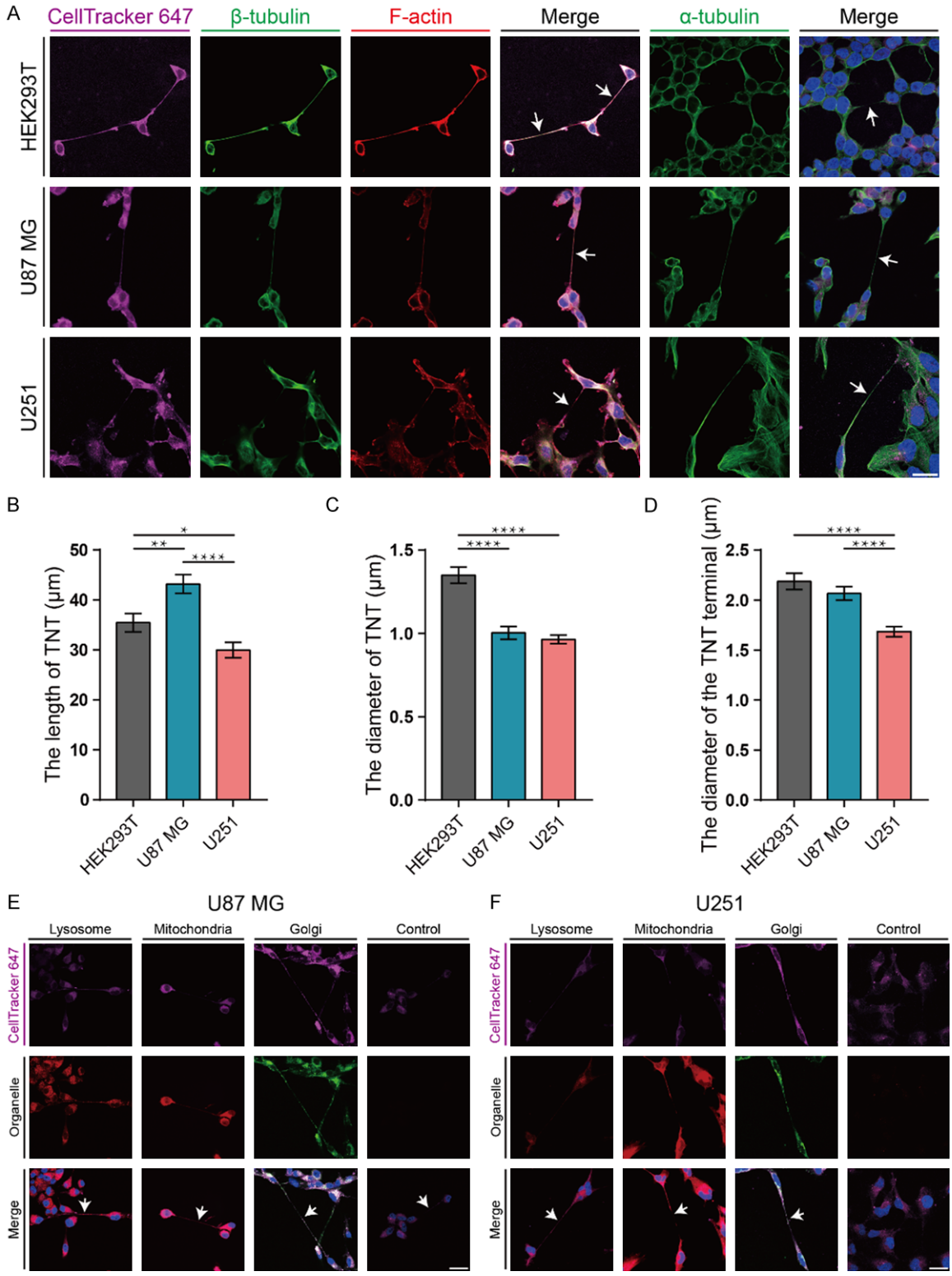

Figure 2. The length, diameter, and cytoskeletal composition of TNTs. TNTs formed by the HEK293T, U87 MG, and U251 cell lines all contained cytoskeletal proteins, including F-actin, α-tubulin, and β-tubulin. The lysosomes, mitochondria, and Golgi bodies in U87 MG and U251 cells were labeled with organelle-specific small-molecule dyes. These organelles were observed in TNTs, which indicated that lysosomes, mitochondria, and Golgi bodies can be transported through TNTs. (A) TNTs formed by HEK293T, U87 MG, and U251 cells contained F-actin, α-tubulin, and β-tubulin. After induction by 100 μmol/L H_2O_2 (HEK293T and U87 MG cells) and 50 μmol/L H_2O_2 (U251 cells), the cells were assessed by immunochemical staining intensity. Purple: CellTracker fluorescent probe. Green: α-tubulin

and β-tubulin. Red: F-actin. Blue: nuclei. Arrowheads: TNTs formed between cells. Objective: 40×, eyepiece: 10×. Scale bar: 10 μm. (B-D) TNTs formed by different cells were of different lengths (B) and diameters (C, D). Length: HEK293T cells (35.44±1.856 μm, n=64), U87 MG cells (43.15±1.875 μm, n=82), and U251 cells (29.96±1.548 μm, n=108). Diameter (middle): HEK293T cells (1.350±0.049 μm, n=64), U87 MG cells (1.004±0.039 μm, n=82), and U251 cells (0.964±0.026 μm), n=108). Diameter (end): HEK293T cells (2.187±0.082 μm, n=64), U87 MG cells (2.067±0.067 μm, n=82), and U251 cells (1.683±0.049 μm, n=108). (E, F) TNT-mediated transport of lysosomes, mitochondria, and Golgi bodies between U87 MG cells (E) and between U251 cells (F). After induction with a working concentration of H_2O_2 for 24 hours, the cells were labeled with CellTracker 647, and organelles were labeled with various organelle-specific small molecule dyes. The labeled cells were observed through immunochemistry. Purple: CellTracker fluorescent probe. Green: specific marker for Golgi bodies. Red: lysosome and mitochondria marker. Blue: DAPI-labeled nuclei. Arrowheads: TNTs formed between cells. Objective: 40×, eyepiece: 10×. Scale bar: 10 μm.

tion, the donor and recipient cells were co-cultured for 48 hours (**Figure 3A**). In both $spGFP_{1-10}$ and Tau-$spGFP_{1-10}$ groups, the green fluorescence signal in the recipient cells changed over time (**Figure 3B-D**). Additionally, in the group in which donor cells were transfected with Tau-$spGFP_{1-10}$, the fluorescence signal emitted from the mCherry that had been transfected in the donor cells was observed in the recipient cells (**Figure 3D**). Using the initial intensity of the green fluorescence in the recipient cells as the baseline, we analyzed the values in the two groups obtained at different times and normalized (**Figure 3B**). The results showed that the green fluorescence emitted from spGFP changed over time, which indicated that $spGFP_{1-10}$ and Tau-$spGFP_{1-10}$ were transported to recipient cells through TNTs. These results suggested that TNTs were involved in the transport of $spGFP_{1-10}$ and Tau-$spGFP_{1-10}$ between donor and recipient cells.

Tau-EGFP fusion protein can be transported between cells through TNTs

We also studied the intercellular transport of Tau protein based on the expression of a Tau-EGFP fusion protein. Twenty-four hours after the transfection of Tau-EGFP and EGFP plasmids into HEK293T cells, green fluorescence from the Tau-EGFP protein was observed in the cell body and in the TNTs (Figure S2A). Western blotting showed obvious bands at approximately 75 kDa, which is the size of the Tau-EGFP fusion protein (Figure S2B). The combined results from a transfection assay and western blotting confirmed that the Tau-EGFP plasmid was successfully expressed. We further explored the transport of Tau-EGFP protein through TNTs using time-lapse imaging of live cells. HEK293T cells transfected with the Tau-EGFP fusion protein were used as donor cells, and cells transfected with mCherry were used as recipient cells. Twenty-four hours after transfection, the donor cells and recipient cells were co-cultured for 48 hours (**Figure 4A**). The results showed that the fluorescence of the Tau-EGFP protein at the termini of the TNTs increased over time (**Figure 4B**). After 10 minutes, the intensity of the green fluorescence signal increased to be 1.5-fold that of the initial intensity (**Figure 4C**). This outcome suggested that, under physiologic conditions, TNTs mediated the transport of the Tau-EGFP protein between HEK293T cells.

Protein aggregates are pathologic markers for many neurodegenerative diseases [20, 21]. Therefore, we studied TNT-mediated transport of Tau protein in cell lines of the nervous system, aiming to provide new insights into the transport of pathogenic proteins in AD. Specifically, we explored the transport of TNT-mediated Tau-EGFP protein in U87 MG and U251 cell lines through live time-lapse imaging. Bidirectional movement of the Tau-EGFP protein through TNTs was observed in both U87 MG and U251 cells, and the movement of the Tau-EGFP protein oscillated with time (**Figure 4E**, **4F**). Statistical analysis of the data showed that in U87 MG and U251 cells, the velocities of anterograde and retrograde transport were not significantly different. However, compared with U87 MG cells, the velocities of both anterograde and retrograde transport of Tau-EGFP in U251 cells were lower (**Figure 4D**). These results demonstrated that TNT-mediated Tau protein transport can be bidirectional between cells of the same lineage, and that the transport velocity may be different in different cell lines.

Extracellular Tau-AF594 protein can be transported between cells through TNTs

We used exogenous fluorescently labeled Tau protein (Tau-AF594) to verify that TNTs can mediate the transport of Tau protein between cells. Different concentrations of Tau-AF594 were added to the culture medium to obtain

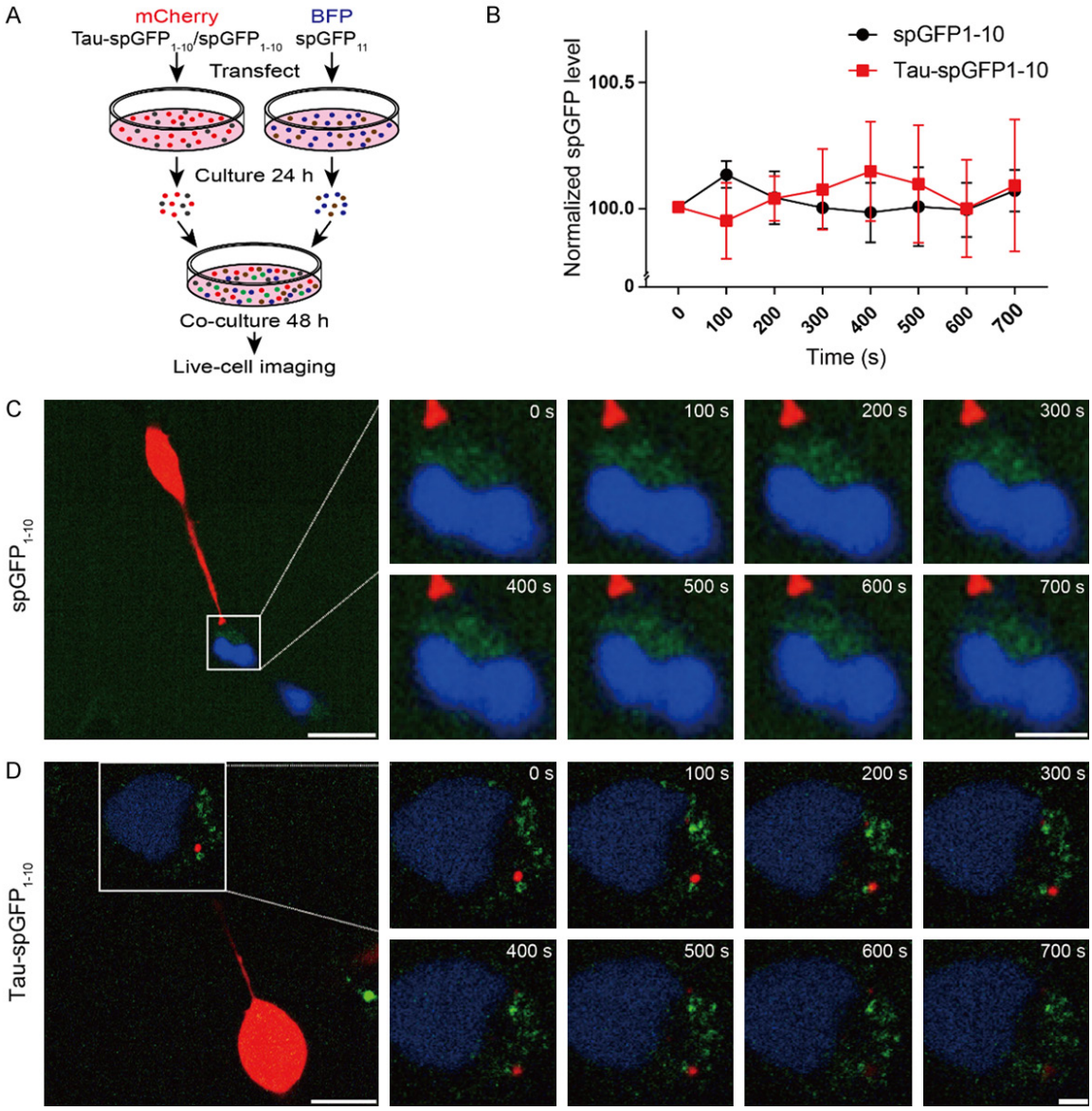

Figure 3. TNTs mediated the transport of the Tau-spGFP fusion protein between HEK293T cells. Donor cells were cotransfected with $spGFP_{1-10}$/Tau-$spGFP_{1-10}$ and mCherry, co-cultured with recipient cells labeled with CellTracker 647, and transfected with $spGFP_{11}$ for 48 hours. Green fluorescence was observed in the recipient cells, and TNTs extended from the donor cells in the two groups, suggesting that the Tau-$spGFP_{1-10}$ protein can be transported between cells through TNTs. (A) Schematic diagram of cocultured donor and recipient cells. $SpGFP_{1-10}$/Tau-$spGFP_{1-10}$ and mCherry were cotransfected into the donor cells. Then, the cells were co-cultured for 48 hours with recipient cells labeled with CellTracker 647 and transfected with $spGFP_{11}$. (B) In the $spGFP_{1-10}$ and Tau-$spGFP_{1-10}$ groups, the green fluorescence in the recipient cells changed over time. With the value of green fluorescence in the recipient cells at the initial time considered the baseline, the values for the two groups at different times were analyzed after normalization. N=3 in each experiment. Two-way ANOVA. (C, D) Time-lapse image of live cells after co-culturing the donor cells transfected with mCherry and $spGFP_{1-10}$ (C)/Tau-$spGFP_{1-10}$ (D) with recipient cells transfected with BFP and $spGFP_{11}$. Objective: 63×, eyepiece: 10×. Scale bars: 30 μm (left) and 10 μm (right).

the optimal working concentration of Tau-AF594 in U87 MG and U251 cells (Figure S3A, S3B). To demonstrate that Tau protein can be transported between cells through TNTs, we transfected cells with EGFP and incubated them with Tau-AF594 protein, considering them donor cells, and then, we cocultured these donor cells with CellTracker 647-labeled recipient cells for 48 hours (**Figure 5A**). Then, Tau-AF594 fluorescence was observed in the TNTs

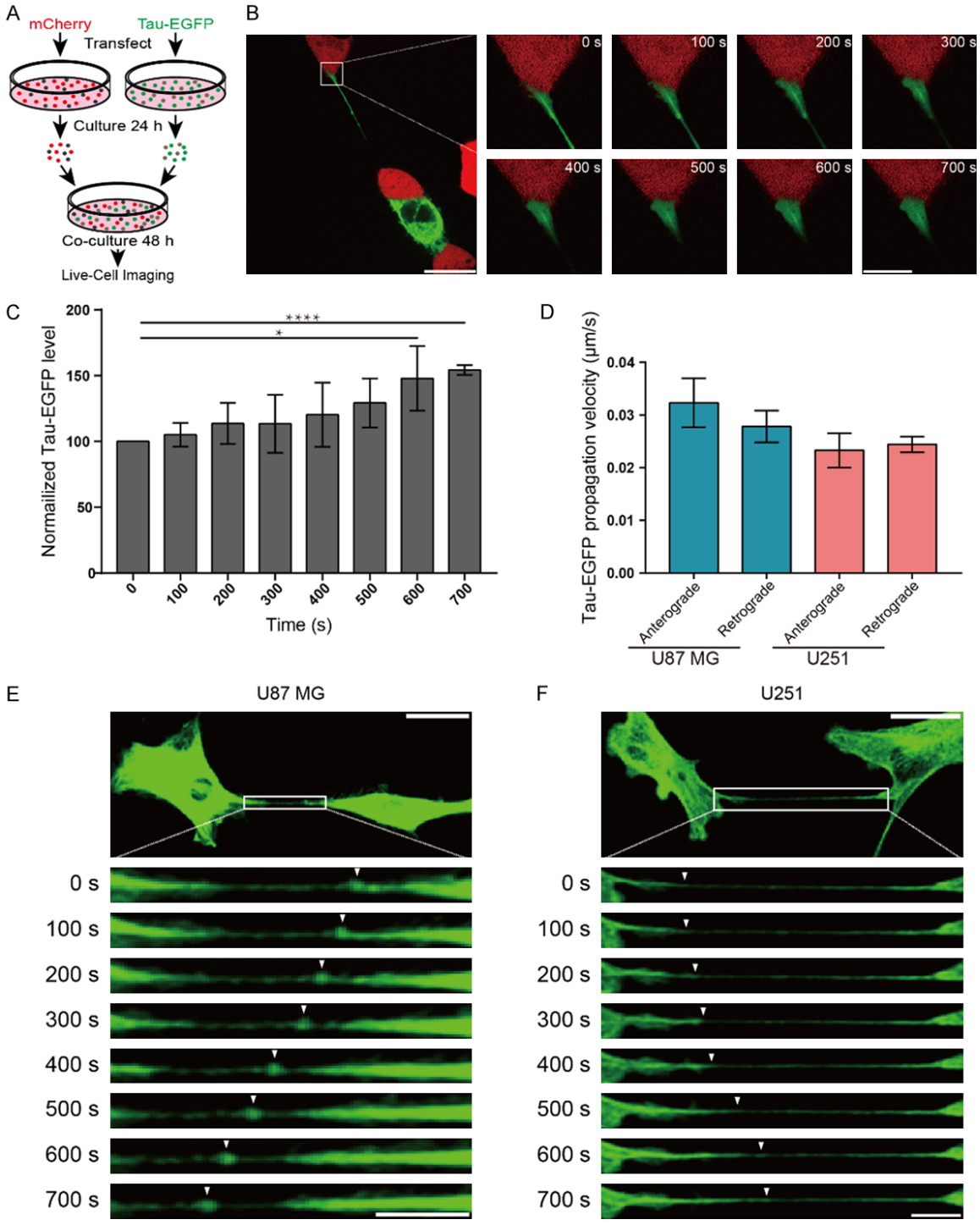

Figure 4. TNTs mediated the transport of the Tau-EGFP fusion protein between HEK293T cells, between U87 MG cells, and between U251 cells. Twenty-four hours after transfection of Tau-EGFP and EGFP plasmids in HEK293T cells, green fluorescence emitted from the Tau-EGFP protein was observed in the cell body and TNTs, indicating that the TNTs mediated Tau-EGFP fusion protein transport. (A) Schematic diagram of the co-cultured donor and recipient cells. HEK293T cells transfected with Tau-EGFP were used as donor cells, and cells transfected with mCherry were used as recipient cells. (B) The green fluorescence (Tau-EGFP) at the junction of the TNT terminals with cells increased over time. The value of the green fluorescence intensity in the TNT terminals at the initial time was used as the standard, and the value at different times was analyzed after normalization. Objective: 63×, eyepiece: 10×. Scale bar: 30 μm (left) and 10 μm (right). (C) Time-lapse image of Tau-EGFP accumulating in the terminals of the TNTs formed by HEK293T cells. The data were obtained from three independent experiments, N=3, t test, *P<0.05,

**P<0.01, ***P<0.001, ****P<0.0001. (D) The anterograde and retrograde transport velocities of Tau-EGFP were not significantly different in the U87 MG and U251 cells (U87 MG cells, anterograde was 0.0323±0.0047 μm/s, n=15, and retrograde was 0.0278±0.0030 μm/s, n=21; U251 cells, anterograde was 0.0233±0.0033 μm/s, n=19, and retrograde was 0.0244±0.0015 μm/s, n=41). (E, F) Tau-EGFP was transported through TNTs between U87 MG (E) and between U251 (F) cells. Arrowheads, fluorescence emitted from Tau-EGFP. Objective: 63×, eyepiece: 10×. Scale bars: 30 μm (top) and 10 μm (bottom).

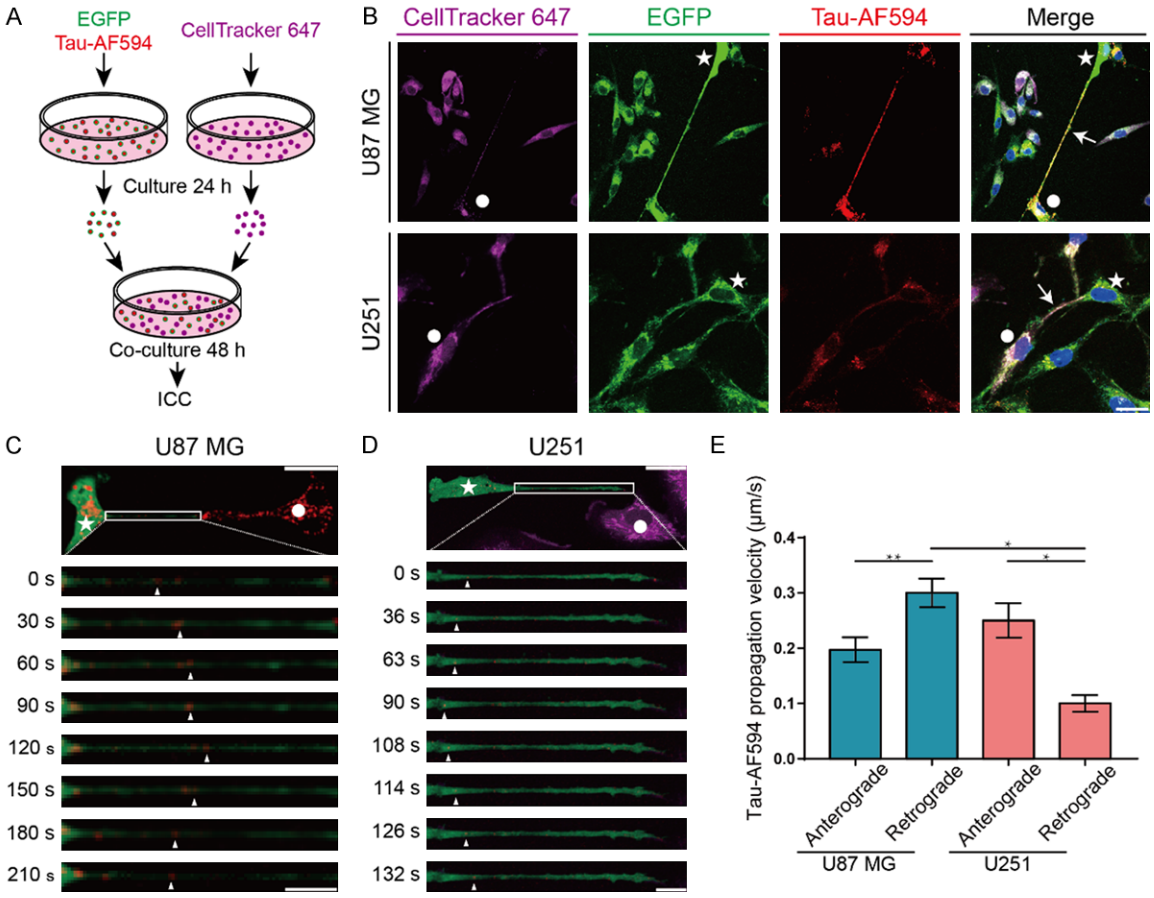

Figure 5. TNTs mediated the bidirectional transport of extracellular Tau-AF594 protein between U87 MG cells and between U251 cells. Cells that were transfected with EGFP and incubated with Tau-AF594 protein were used as donor cells, and these donor cells were cocultured with CellTracker 647-labeled recipient cells for 48 hours. Tau-AF594 protein transported bidirectionally was observed in the TNTs, and the transport velocity of the Tau-AF594 protein was significantly different because of the different properties of the TNTs in different cells. Pentacle, donor cells; circle, recipient cells. A. Schematic diagram of cocultured donor and recipient cells. Cells that were transfected with EGFP and incubated with Tau-AF594 protein were used as donor cells, and they were cocultured with CellTracker 647-labeled recipient cells for 48 hours. B. Red fluorescence (Tau-AF594) was observed in the TNTs and in recipient cells, suggesting that Tau-AF594 was transported from the donor to recipient cells through TNTs. Purple fluorescence in the recipient cells was observed in the TNTs of the U87 MG and U251 cells, suggesting that TNTs mediated the bidirectional transport of materials between the U87 MG cells and between the U251 cells. Purple: CellTracker fluorescent probe. Green: EGFP. Red: Tau protein. Blue: nuclei. Arrowheads: TNTs formed between cells. Objective: 40×, eyepiece: 10×. Scale bar: 10 μm. C. Time-lapse image of TNT-mediated bidirectional transport of Tau-AF594 in U87 MG cells. Green: EGFP. Red: Tau protein. Arrowheads: fluorescence emitted from Tau-AF594. Objective: 63×, eyepiece: 10×. Scale bars: 30 μm (top) and 10 μm (bottom). D. Time-lapse image of TNT-mediated bidirectional transport of Tau-AF594 between U251 cells. Green: EGFP. Red: Tau protein. Purple: CellTracker fluorescent probe. Arrowheads: fluorescence emitted from Tau-AF594. Objective: 63×, eyepiece: 10×. Scale bars: 30 μm (top) and 10 μm (bottom). E. The retrograde transport velocity of Tau-AF594 was increased in U87 MG cells and decreased in U251 cells. (U87 cells, anterograde was 0.1972±0.0227 μm/s, n=30, and retrograde was 0.2894±0.0260 μm/s, n=49; U251 cells, anterograde was 0.2502±0.0312 μm/s, n=17, and retrograde was 0.1002±0.0150 μm/s, n=5). The data were obtained from three independent experiments, t test, *P<0.05, **P<0.01, ***P<0.001, ****P<0.0001.

and recipient cells of both the U87 MG and U251 lineage (**Figure 5B**). The results demonstrated that Tau-AF594 was transported from donor to recipient cells through TNTs. Furthermore, purple fluorescence emitted by the recipient cells was observed in TNTs, suggesting that TNTs mediate the bidirectional transport of substances between U87 MG and between U251 cells.

To explore the intercellular transport process mediated by TNTs under physiologic conditions, time-lapse imaging of live cells was performed. Red fluorescence emitted by the Tau-AF594 protein was observed in TNTs in both the U87 MG and U251 cell lines (**Figure 5C**, **5D**). Similar to previous studies, the Tau-AF594 protein was transported bidirectionally through TNTs. A comparison between U87 MG and U251 cells revealed no significant difference in the velocity of anterograde Tau-AF594 transport through the TNTs, but the velocity of retrograde transport was significantly higher through the TNTs of the U87 MG cells (**Figure 5E**). This finding suggested that the Tau-AF594 protein can be transported bidirectionally through TNTs and that the velocity of Tau-AF594 anterograde and retrograde transport significantly differed. The transport velocity of the Tau-AF594 protein varied significantly due to the different properties of the TNTs formed by different cells.

TNTs can mediate the transport of Aβ-AF594 between cells

In addition to the Tau protein, aggregation of Aβ is one of the most common pathologies in AD [27]. In the Aβ hypothesis, Aβ dimers, oligomers, and plaques are the pathogenic sources of AD. However, how Aβ is transported over long distances across different regions has not been determined. Here, we used exogenous fluorescently labeled Aβ (Aβ-AF594) to investigate whether Aβ can be transported through TNTs. Similar to our Tau-AF594 experiments, the working concentration of Aβ-AF594 was first established (Figure S3C, S3D). Then, we used cells that were transfected with EGFP and incubated with Aβ-AF594 as donor cells and cocultured them with CellTracker 647-labeled recipient cells for 48 hours (**Figure 6A**). Red fluorescence signals were observed in the TNTs formed by both U87 MG and U251 cells and in recipient cells (**Figure 6B**), suggesting that Aβ-AF594 was transported from donor to recipient cells through TNTs. Time-lapse imaging of living cells showed that Aβ-AF594 emitted red fluorescence in both U87 MG and U251 cells (**Figure 6C**, **6D**). Similar to previous studies, the transport of Aβ-AF594 was found to be bidirectional through the TNTs. We also found that the transport velocity of Aβ-AF594 anterograde and retrograde transport through the TNTs did not significantly differ between the U87 MG and between the U251 cells (**Figure 6E**).

Discussion

Increasing evidence suggests that the remarkable pathology of many neurodegenerative diseases is based on the accumulation of pathogenic proteins in the brain [21]. Spreading of protein aggregates in the brain is also believed to be related to the pathologic progression of neurodegenerative diseases. In addition, it has been reported that mutant huntingtin (mHTT) can promote the formation of TNTs, thus providing an effective mechanism for mHTT transport between neuronal cells and primary neurons [33]. Most importantly, different disease-associated proteins (including Aβ, Tdp43, and Tau protein) have been found to support TNT-mediated transport of pathogenic protein aggregates [18, 24-26]. Taken together, these results suggest that TNT transportation may be a common mechanism in the progression of neurodegenerative diseases, providing a target for the treatment of these diseases. Although the transport of aggregates through TNTs in some cell lines has been demonstrated, neither the function of TNTs formed by neurons nor the function of the interneuronal aggregation of the proteins transported through TNTs is clear. The key of developing therapeutic strategies to slow disease progression is understanding whether and how TNTs are formed in neurons. In addition, searching for specific molecular markers of TNTs and verifying the functions of TNT-mediated material transport and signal transduction in primary neurons, glial cells, and other cell lines are problems to be solved through research. When TNTs can be specifically labeled, their functions can be further studied in vivo.

Here, we studied the transport of the Tau protein and Aβ through TNTs. We first investigated TNT-mediated transport of Tau-spGFP$_{1-10}$, Tau-EGFP, Tau-AF594 and Aβ-AF594 in HEK293T cells and later validated our results in human astroblastoma U87 MG and human glioma

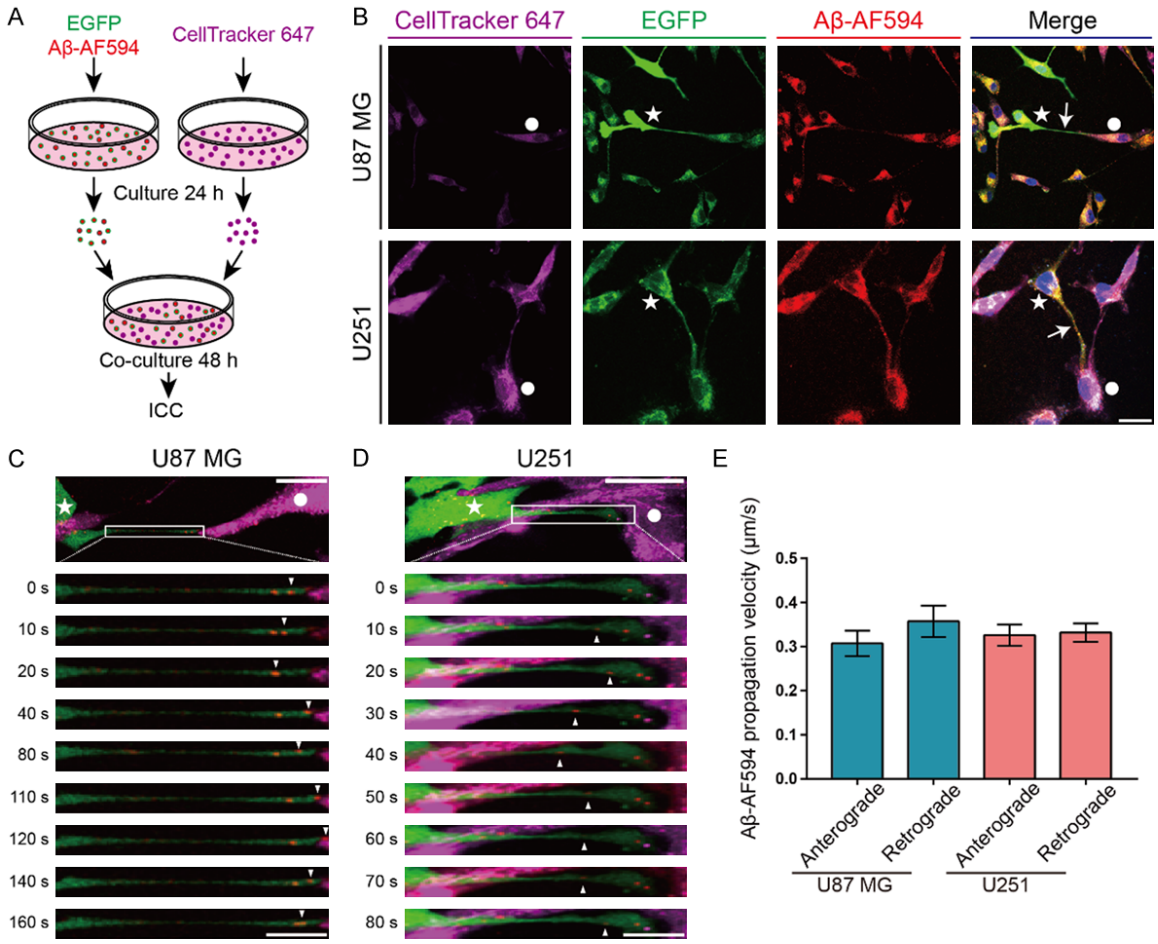

Figure 6. TNTs mediated bidirectional transport of extracellular Aβ-AF594 between U87 MG cells and between U251 cells. Cells that were transfected with EGFP and incubated with Aβ-AF594 were used as donor cells and then cocultured with CellTracker 647-labeled recipient cells for 48 hours. Bidirectional Aβ-AF594 transport was observed in the TNTs, and the transport velocity of Tau-AF594 was not significantly different between U87 MG and U251 cells. Pentacle, donor cells; circle, recipient cells. A. Schematic diagram of co-cultured donor and recipient cells. Cells that were transfected with EGFP and incubated with Aβ-AF594 were used as donor cells, and they were co-cultured with CellTracker 647-labeled recipient cells for 48 hours. B. Red fluorescence (Aβ-AF594) was observed in the TNTs and recipient cells, suggesting that Aβ-AF594 was transported from donor to recipient cells through TNTs. Purple fluorescence in the recipient cells was observed in TNTs formed by U87 MG and U251 cells, suggesting that TNTs mediated bidirectional transport of materials between U87 MG cells and between U251 cells. Purple: CellTracker fluorescent probe. Green: EGFP. Red: Aβ. Blue: nuclei. Arrowheads: TNTs formed between cells. Objective: 40×, eyepiece: 10×. Scale bar: 10 μm. C. Time-lapse image of TNT-mediated bidirectional transport of Aβ-AF594 between U87 MG cells. Green: EGFP. Red: Aβ. Arrowheads: fluorescence emitted from Aβ-AF594. Objective: 63×, eyepiece: 10×. Scale bars: 30 μm (top) and 10 μm (bottom). D. Time-lapse image of TNT-mediated bidirectional transport of Aβ-AF594 between U251 cells. Green: EGFP. Red: Aβ. Purple: CellTracker fluorescent probe. Arrowheads: fluorescence emitted from Aβ-AF594. Objective: 63×, eyepiece: 10×. Scale bars: 30 μm (top) and 10 μm (bottom). E. The anterograde and retrograde transport velocities of Aβ-AF594 were not significantly different in either U87 MG or U251 cells. (U87 MG cells, anterograde was 0.3071±0.0288 μm/s, n=54, and retrograde was 0.3574±0.0353 μm/s, n=38; U251 cells, anterograde was 0.3260±0.0242 μm/s, n=57, and retrograde was 0.3319±0.0208 μm/s, n=69). The data were obtained from three independent experiments, t test, *P<0.05, **P<0.01, ***P<0.001, ****P<0.0001.

U251. Our results indicated that TNTs formed by different cell lines can mediate the transport of different forms of Tau protein and Aβ.

Importantly, we found that both the Tau protein and Aβ can be transported bidirectionally in different cell lines, and the velocity of Tau protein transportation varies significantly in different cell lines. For the Tau-EGFP fusion protein, the velocities of anterograde and retrograde transport were 0.0323±0.0047 μm/s and 0.0278±0.0030 μm/s in U87 MG cells and 0.0233±

0.0033 μm/s and 0.0244±0.0015 μm/s in U251 cells, respectively. There were no significant differences between the four groups. However, for Tau protein uptake directly from cell culture medium, the velocities of anterograde and retrograde transport were 0.1972± 0.0227 μm/s and 0.2894±0.0260 μm/s in U87 MG cells and 0.2502±0.0312 μm/s and 0.1002±0.0150 μm/s in U251 cells, respectively. These results showed that compared with the overexpressed Tau-EGFP fusion protein, the velocity of Tau protein uptake directly from the culture medium was nearly ten-fold faster through TNTs. Similarly, for direct uptake of Aβ, the velocity of transport in different cell lines was also faster, by several orders of magnitude, than that of the overexpressed Tau-EGFP fusion protein. Therefore, we speculated that under pathologic AD conditions, after the cascade of cell death, the excess phosphorylated Tau protein and Aβ in cells are released outside the cell. The surrounding cells take up these aggregates and expedite the progression of AD by rapidly and directly transporting the Tau protein or Aβ to surrounding cells through TNTs.

Hyperphosphorylated Tau protein and Aβ are known to induce the accumulation of a large number of intracellular-related proteins when they are transported to secondary cells, thus accelerating the apoptosis of neurons. Our findings demonstrated the intercellular transport of the Tau protein and Aβ and provided a plausible explanation for the cascade of neuronal death in the brain during the progression of AD.

Acknowledgements

This work was supported by the National Science Foundation of China (NSFC) major research grant (31630028) and NSFC general research grant (81971679). We also thank the staff at the National Center for Protein Sciences, the Core Facilities of the School of Life Sciences and the State Key Laboratory of Membrane Biology at Peking University for their assistance.

Disclosure of conflict of interest

None.

Address correspondence to: Dr. Yan Zhang, College of Life Sciences, Room 412, Peking University, Beijing 100871, China. Tel: +86-10-62754880; Fax: +86-10-62751526; E-mail: yanzhang@pku.edu.cn

References

[1] Lucas WJ, Ham BK and Kim JY. Plasmodesmata-bridging the gap between neighboring plant cells. Trends Cell Biol 2009; 19: 495-503.

[2] Abounit S and Zurzolo C. Wiring through tunneling nanotubes–from electrical signals to organelle transfer. J Cell Sci 2012; 125: 1089-1098.

[3] Rustom A, Saffrich R, Markovic I, Walther P and Gerdes HH. Nanotubular highways for intercellular organelle transport. Science 2004; 303: 1007-1010.

[4] Sisakhtnezhad S and Khosravi L. Emerging physiological and pathological implications of tunneling nanotubes formation between cells. Eur J Cell Biol 2015; 94: 429-443.

[5] Gerdes HH and Carvalho RN. Intercellular transfer mediated by tunneling nanotubes. Curr Opin Cell Biol 2008; 20: 470-475.

[6] Zhang J and Zhang Y. Membrane nanotubes: novel communication between distant cells. Sci China Life Sci 2013; 56: 994-999.

[7] Eugenin EA, Gaskill PJ and Berman JW. Tunneling nanotubes (TNT) are induced by HIV-infection of macrophages: a potential mechanism for intercellular HIV trafficking. Cell Immunol 2009; 254: 142-148.

[8] Gousset K, Schiff E, Langevin C, Marijanovic Z, Caputo A, Browman DT, Chenouard N, de Chaumont F, Martino A, Enninga J, Olivo-Marin JC, Männel D and Zurzolo C. Prions hijack tunnelling nanotubes for intercellular spread. Nat Cell Biol 2009; 11: 328-336.

[9] Kumar A, Kim JH, Ranjan P, Metcalfe MG, Cao W, Mishina M, Gangappa S, Guo Z, Boyden ES, Zaki S, York I, García-Sastre A, Shaw M and Sambhara S. Influenza virus exploits tunneling nanotubes for cell-to-cell spread. Sci Rep 2017; 7: 40360.

[10] Wang X, Veruki ML, Bukoreshtliev NV, Hartveit E and Gerdes HH. Animal cells connected by nanotubes can be electrically coupled through interposed gap-junction channels. Proc Natl Acad Sci U S A 2010; 107: 17194-17199.

[11] Rustom A. The missing link: does tunnelling nanotube-based supercellularity provide a new understanding of chronic and lifestyle diseases? Open Biol 2016; 6: 160057.

[12] Acquistapace A, Bru T, Lesault PF, Figeac F, Coudert AE, le Coz O, Christov C, Baudin X, Auber F, Yiou R, Dubois-Randé JL and Rodriguez AM. Human mesenchymal stem cells reprogram adult cardiomyocytes toward a progenitor-like state through partial cell fusion and mitochondria transfer. Stem Cells 2011; 29: 812-824.

[13] Koyanagi M, Brandes RP, Haendeler J, Zeiher AM and Dimmeler S. Cell-to-cell connection of endothelial progenitor cells with cardiac myocytes by nanotubes: a novel mechanism for cell fate changes? Circ Res 2005; 96: 1039-1041.
[14] Liu K, Ji K, Guo L, Wu W, Lu H, Shan P and Yan C. Mesenchymal stem cells rescue injured endothelial cells in an in vitro ischemia-reperfusion model via tunneling nanotube like structure-mediated mitochondrial transfer. Microvasc Res 2014; 92: 10-18.
[15] Takahashi A, Kukita A, Li YJ, Zhang JQ, Nomiyama H, Yamaza T, Ayukawa Y, Koyano K and Kukita T. Tunneling nanotube formation is essential for the regulation of osteoclastogenesis. J Cell Biochem 2013; 114: 1238-1247.
[16] Whitehead J, Zhang J, Harvestine JN, Kothambawala A, Liu GY and Leach JK. Tunneling nanotubes mediate the expression of senescence markers in mesenchymal stem/stromal cell spheroids. Stem Cells 2020; 38: 80-89.
[17] Rostami J, Holmqvist S, Lindström V, Sigvardson J, Westermark GT, Ingelsson M, Bergström J, Roybon L and Erlandsson A. Human astrocytes transfer aggregated alpha-synuclein via tunneling nanotubes. J Neurosci 2017; 37: 11835-11853.
[18] Tardivel M, Bégard S, Bousset L, Dujardin S, Coens A, Melki R, Buée L and Colin M. Tunneling nanotube (TNT)-mediated neuron-to neuron transfer of pathological Tau protein assemblies. Acta Neuropathol Commun 2016; 4: 117.
[19] Wang J, Liu X, Qiu Y, Shi Y, Cai J, Wang B, Wei X, Ke Q, Sui X, Wang Y, Huang Y, Li H, Wang T, Lin R, Liu Q and Xiang AP. Cell adhesion-mediated mitochondria transfer contributes to mesenchymal stem cell-induced chemoresistance on T cell acute lymphoblastic leukemia cells. J Hematol Oncol 2018; 11: 11.
[20] Dewey CM, Cenik B, Sephton CF, Johnson BA, Herz J and Yu G. TDP-43 aggregation in neurodegeneration: are stress granules the key? Brain Res 2012; 1462: 16-25.
[21] Victoria GS and Zurzolo C. The spread of prion-like proteins by lysosomes and tunneling nanotubes: implications for neurodegenerative diseases. J Cell Biol 2017; 216: 2633-2644.
[22] Scheckel C and Aguzzi A. Prions, prionoids and protein misfolding disorders. Nat Rev Genet 2018; 19: 405-418.
[23] Abounit S, Bousset L, Loria F, Zhu S, de Chaumont F, Pieri L, Olivo-Marin JC, Melki R and Zurzolo C. Tunneling nanotubes spread fibrillar α-synuclein by intercellular trafficking of lysosomes. EMBO J 2016; 35: 2120-2138.
[24] Abounit S, Wu JW, Duff K, Victoria GS and Zurzolo C. Tunneling nanotubes: a possible highway in the spreading of tau and other prion-like proteins in neurodegenerative diseases. Prion 2016; 10: 344-351.
[25] Ding X, Ma M, Teng J, Teng RK, Zhou S, Yin J, Fonkem E, Huang JH, Wu E and Wang X. Exposure to ALS-FTD-CSF generates TDP-43 aggregates in glioblastoma cells through exosomes and TNTs-like structure. Oncotarget 2015; 6: 24178-24191.
[26] Wang Y, Cui J, Sun X and Zhang Y. Tunneling-nanotube development in astrocytes depends on p53 activation. Cell Death Differ 2011; 18: 732-742.
[27] Lee VM, Goedert M and Trojanowski JQ. Neurodegenerative tauopathies. Annu Rev Neurosci 2001; 24: 1121-1159.
[28] Yamashita YM, Inaba M and Buszczak M. Specialized intercellular communications via cytonemes and nanotubes. Annu Rev Cell Dev Biol 2018; 34: 59-84.
[29] Bukoreshtliev NV, Wang X, Hodneland E, Gurke S, Barroso JF and Gerdes HH. Selective block of tunneling nanotube (TNT) formation inhibits intercellular organelle transfer between PC12 cells. FEBS Lett 2009; 583: 1481-1488.
[30] Dilsizoglu Senol A, Pepe A, Grudina C, Sassoon N, Reiko U, Bousset L, Melki R, Piel J, Gugger M and Zurzolo C. Effect of tolytoxin on tunneling nanotube formation and function. Sci Rep 2019; 9: 5741.
[31] Panasiuk M, Rychłowski M, Derewońko N and Bieńkowska-Szewczyk K. Tunneling nanotubes as a novel route of cell-to-cell spread of herpesviruses. J Virol 2018; 92: e00090-18.
[32] Wang X and Gerdes HH. Transfer of mitochondria via tunneling nanotubes rescues apoptotic PC12 cells. Cell Death Differ 2015; 22: 1181-1191.
[33] Costanzo M, Abounit S, Marzo L, Danckaert A, Chamoun Z, Roux P and Zurzolo C. Transfer of polyglutamine aggregates in neuronal cells occurs in tunneling nanotubes. J Cell Sci 2013; 126: 3678-3685.

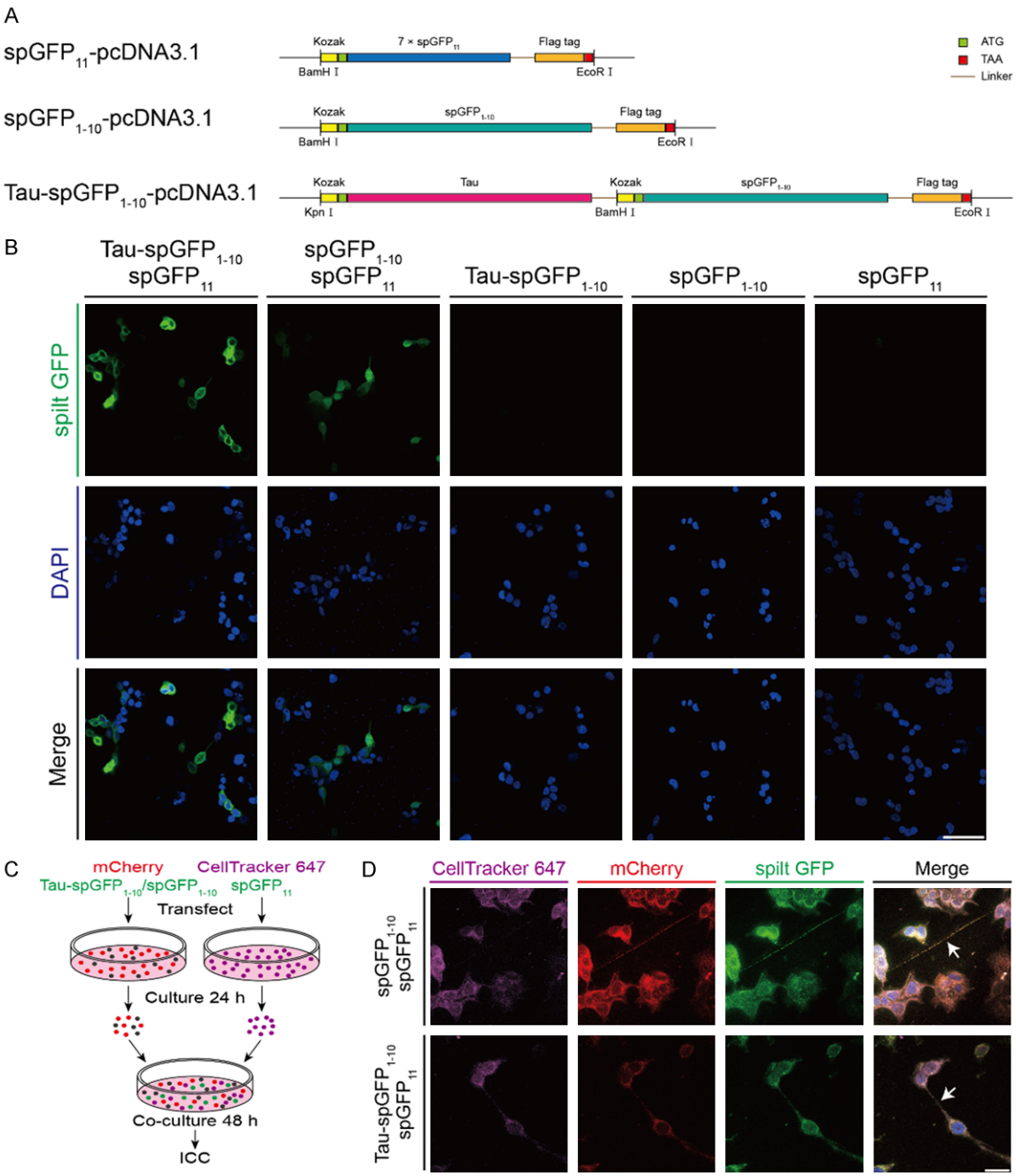

Figure S1. Construction and verification of the Tau-spGFP$_{1-10}$-pcDNA3.1 plasmid. A. Construction of Tau-spGFP$_{1-10}$, spGFP$_{1-10}$, and spGFP$_{11}$. B. The Tau-spGFP$_{1-10}$, spGFP$_{1-10}$, and spGFP$_{11}$ plasmids were successfully expressed in HEK293T cells. Green: spGFP fluorescence signal. Blue: nuclei. Objective: 10×, eyepiece: 10×. Scale bar: 50 μm. C. Schematic diagram of co-cultured donor cells transfected with mCherry and Tau-spGFP$_{1-10}$/spGFP$_{1-10}$ and recipient cells transfected with spGFP$_{11}$ and labeled with CellTracker 647. D. Green fluorescence was observed in the TNTs and in recipient cells. Purple: CellTracker fluorescent probe. Green: spGFP. Red: mCherry. Blue: nuclei. Arrowheads: TNTs formed between cells. Objective: 40×, eyepiece: 10×. Scale bar: 10 μm.

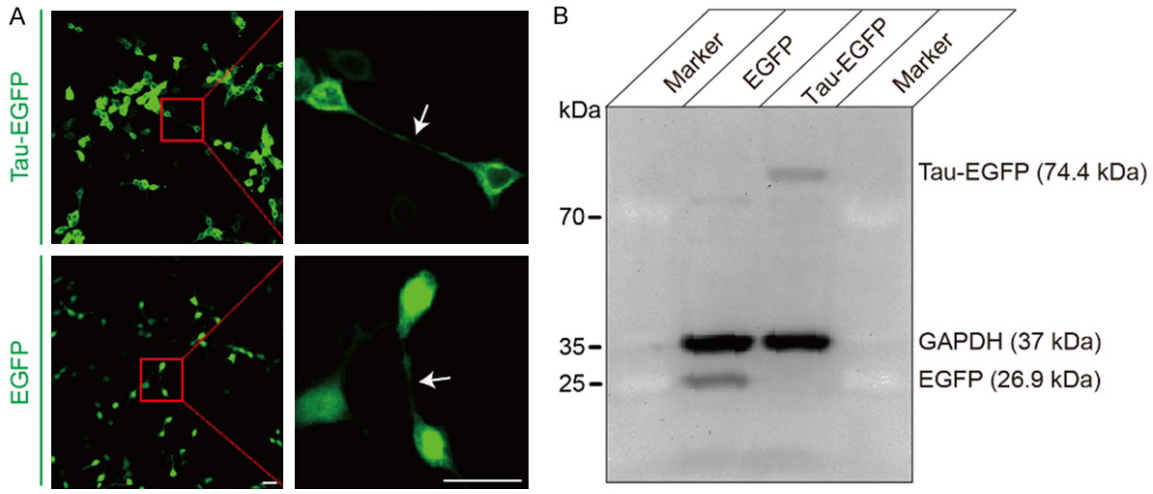

Figure S2. Tau-EGFP plasmid was successfully expressed in HEK293T cells. A. Fluorescence image showing that the Tau-EGFP plasmid was successfully expressed in HEK293T cells. After transfection of Tau-EGFP and EGFP in HEK293T cells, the green fluorescence emitted by Tau-EGFP was observed in the cell body and TNTs. Arrowheads: TNTs formed between cells. Objective: 10×, eyepiece: 10×. Scale bar: 25 μm. B. Western blot analysis showed that the Tau-EGFP plasmid was successfully expressed.

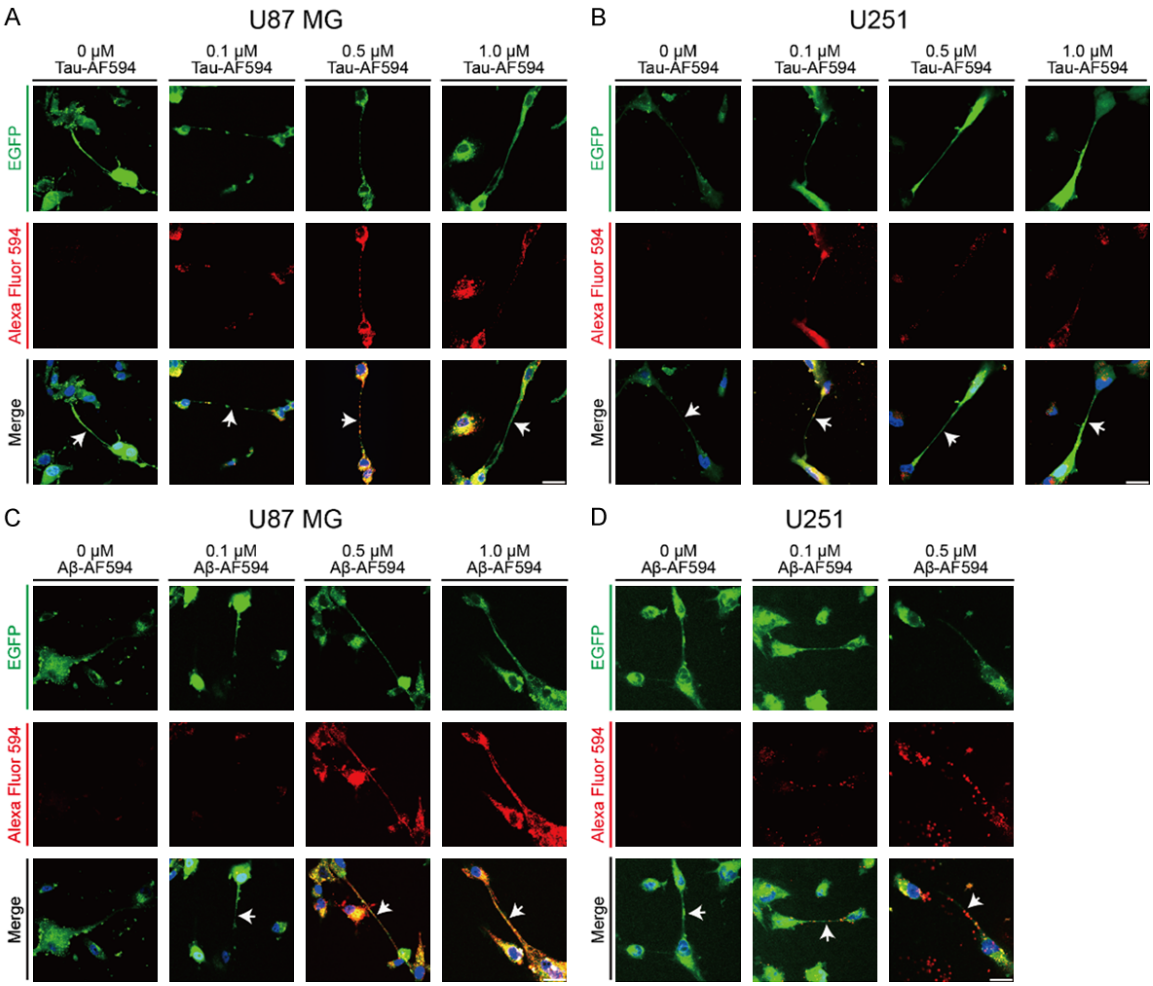

Figure S3. Tau-AF594 and Aβ-594 incubation with U87 MG and U251 cells. (A, B) U87 MG cells (A) and U251 cells (B) were incubated with 0, 0.1, 0.5, and 1.0 μM Tau-AF594, and the optimal working concentration was determined to be 0.1 μM. Red: Tau protein. Blue: nuclei. Green: EGFP. Arrowheads: TNTs formed between cells. Objective: 40×, eyepiece: 10×. Scale bar: 10 μm. (C, D) U87 MG cells (C) and U251 cells (D) were incubated with 0, 0.1, 0.5, and 1.0 μM Aβ-AF594, and the optimal working concentration was determined to be 0.5 μM. Red: Aβ. Blue: nuclei. Green: EGFP. Arrowheads: TNTs formed between cells. Objective: 40×, eyepiece: 10×. Scale bar: 10 μm.